Thermodynamics of ultra-thin oxide overgrowths on Al–Mg alloys: Role of interface energy

D. Ajmera, E. Panda*

Department of Materials Science & Engineering, Indian Institute of Technology Gandhinagar, 382424 Chandkheda, Ahmedabad, India

A B S T R A C T

A thermodynamic model is developed to predict the ultra-thin crystalline oxide overgrowth due to dry, thermal oxidation of single crystalline ⟨AlMg⟩ alloy substrate with respect to various parameters. Along with the bulk Gibbs free energies, this model also took the alloy/oxide interface energies and oxide surface energies into consideration. The developed model was then compared with the amorphous oxide overgrowths on this alloy substrate. For all cases, stability of a particular oxide at lower oxide-film thicknesses is found to be due to its lower interface and surface energies. The model predictions are found to be at par with the experimental observations.

© 2015 Elsevier Ltd. All rights reserved.

1. Introduction

Microstructure of an ultra-thin (≤5 nm) oxide film grown on a metal or metallic alloy substrate defines its functionalities, such as, strength, stiffness, wettability, electrical conductivity, optical transmittance, etc, as a result, controlling the structure-property correlation of the entire system and so its potential applications in areas, like, catalysis, chemical sensors, microelectronic, magnetic devices, wear and corrosion coatings [1–8]. As a consequence, it is extremely essential to understand these microstructures for tuning their properties in these applications.

Microstructure of this ultra-thin oxide-film can be notably different from a thicker one, because of the dominance of the interface energies over the bulk Gibbs free energy in stabilizing an oxide phase at lower oxide-film thicknesses [9–15]. Note that the thickness-dependent bulk Gibbs free energy term becomes substantial at higher oxide-film thicknesses, thus influencing its phase and eventually microstructure. A detailed thermodynamic analysis predicting the growth of an ultra-thin oxide phase (between the amorphous and crystalline oxides) due to dry, thermal oxidation of bare metal substrates is available in literature [9–11]. However, reports of similar kind on a binary alloy substrate are limited. Additionally, in these studies only growth of amorphous oxides have been considered [14,15]. Moreover, a unique thermodynamic formalism predicting the most stable oxide overgrowth among its all

possible amorphous and crystalline oxides due to dry, thermal oxidation of a binary alloy substrate has not been attempted so far. Developing this formalism is extremely relevant, as for the case of some metal oxides (i.e., MgO on Mg, Cu_2O on Cu, etc [11]), a crystalline oxide (rather than an amorphous one) starts to form from the beginning of the oxide growth. Moreover, in case of oxidation of a binary alloy, oxidation-induced chemical segregation of one of the alloying species at the alloy/oxide interface may completely alter the alloy surface and sub-surface constitution, hence, altering the thermodynamics of the entire system [14,16,17].

In particular, for the oxidation of a binary alloy substrate, such as, Al–Mg alloy, where, both the alloying elements (i.e., Al and Mg) have stronger affinity for oxygen, it is very difficult to predict the oxide microstructure under various growth conditions. This is unlike the alloy systems, such as, Au–Cu and Al–Pt, where, one alloying element is nobler than the other, thus, forming an oxide-film consisting of the less noble alloying species. Moreover, Al–Mg alloys have technological importance due to their good weldability, formability, higher strength-to-weight ratio and high ductility, thus finding applicability in automotive parts, cryogenic tanks, marine engine products, etc [18–20]. However, deterioration of these alloys has been a concern, with substantial amount of research focusing on the improvement of oxidation resistance of these alloys, either by the addition of alloying elements or by coating these alloy substrates with a more protective layer [21–23]. Including a different alloying element to the Al–Mg alloys or coating them with different materials may compromise the properties of the original alloys, thus adversely affecting their functionalities for any application [24,25]. Moreover, a complete understanding on the oxidation

⟨⟩   Crystalline solid state
{}   Amorphous solid state
()   Any of the crystalline and/or amorphous solid states
x_{Mg}^i Mg alloying elemental content at the alloy/oxide interface
T Oxide growth temperature
$h_{(oxide)}$ Oxide film thickness for crystalline oxide overgrowth
$V_{<oxide>}$ Molar volume per mole of O of the crystalline oxide at a particular T
V_0 Molar volume of the oxide at $T_0 = 298.15$ K
α Linear thermal expansion coefficient of the oxide
$l_{(oxide)}^2$ Interface area of the crystalline oxide
$G_{<oxide>}^{cell}$ Total Gibbs free energy of the crystalline oxide
$\Delta G_{<oxide>}^f$ Bulk Gibbs free energy of the crystalline oxide formation per mole of oxygen
$\gamma_{<AlMg>-<oxide>}$ Alloy/oxide interface energy for the crystalline oxide overgrowth
$\gamma_{<oxide-ambient>}$ Surface energy of the crystalline oxide
$\gamma_{(AlMg)-(oxide)}^{interaction}$ Chemical interaction contribution to the alloy/oxide interface energy
$\gamma_{(AlMg)-(oxide)}^{geom}$ Geometrical contribution to the alloy/oxide interface energy
$\gamma_{(AlMg)-(oxide)}^{strain}$ Oxide strain energy
$\Delta H_{Al\,in\langle Mg\rangle}^\infty$ Enthalpy of mixing of 1 mol of Al atoms at infinite dilution in ⟨Mg⟩
$\Delta H_{Mg\,in\langle Al\rangle}^\infty$ Enthalpy of mixing of 1 mol of Mg atoms at infinite dilution in ⟨Al⟩
$\Delta H_{O\,in\langle Mg\rangle}^\infty$ Enthalpy of mixing of 1 mol of O atoms at infinite dilution in ⟨Mg⟩
$\Delta H_{O\,in\langle Al\rangle}^\infty$ Enthalpy of mixing of 1 mol of O atoms at infinite dilution in ⟨Al⟩
$A_{(O)}$ Molar interface area of 1 mol of O atoms in the oxide at the alloy/oxide interface
$A_{(Al)}$ Molar interface area of 1 mol of ⟨Al⟩ ions in the oxide at the alloy/oxide interface
$A_{(Mg)}$ Molar interface area of 1 mol of ⟨Mg⟩ ions in the oxide at the alloy/oxide interface
$A_{<AlMg>}^{fcc}$ Molar interface area of 1 mol of the alloy in the substrate at the alloy/oxide interface
$E_{(oxide)}$ Young's modulus of the crystalline oxide
$\nu_{(oxide)}$ Poisson's ratio of the crystalline oxide
ϵ Strain in the oxide film
$a_{(AlMg)}$ Unstrained lattice parameter of the ⟨AlMg⟩ alloy substrate
$a_{(oxide)}$ Unstrained lattice parameter of the oxide
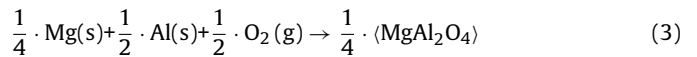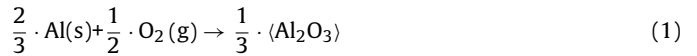$h_{<oxide>}^{critical}$ Critical oxide-film thickness

behaviour of these alloys under various operating conditions would help in designing materials for specific applications.

Thus, in this study, a thermodynamic analysis is presented to predict the growth of epitaxial crystalline oxides (i.e., ⟨Al₂O₃⟩, ⟨MgO⟩ and ⟨MgAl₂O₄⟩) on ⟨AlMg⟩ alloy substrate as a function of Mg alloying elemental content at the alloy/oxide interface $\left(\text{i.e., } 0 \leq x_{Mg}^i \leq 0.5\right)$, growth temperature ($T$ varying in the range of 298.15–900 K), oxide film thickness (up to 5 nm) and low-index crystallographic surfaces of the alloy substrate. Along with the bulk Gibbs free energies of these oxides, this model also considered alloy/oxide interface energies and oxide surface energies for cal-

culating the total Gibbs energies. This developed model was then compared with the existing thermodynamic analysis for the growth of amorphous oxides (i.e., {Al₂O₃}, {MgO} and {MgAl₂O₄}) on this alloy substrate to predict the thermodynamically most preferred oxide overgrowth. Finally, these model predictions are experimentally validated with available literature data.

2. Thermodynamic basis of the model: energy contributions

To predict which of the pure single phase crystalline oxide overgrowths (⟨Al₂O₃⟩, ⟨MgO⟩ or ⟨MgAl₂O₄⟩) is preferred thermodynamically on a single-crystalline ⟨AlMg⟩ alloy substrate due to dry, thermal oxidation, total Gibbs free energies of these oxide films $\left(G_{(oxide)}^{cell}\right)$ are calculated and compared assuming the growth of continuous, homogeneous and isotropic films of uniform thickness, $h_{(oxide)}$. Here, oxide-film growth has been considered in 1-D $h_{(oxide)}$ direction only. Further, this formalism has not taken the kinetic aspects of the oxide growth (i.e., rates of physisorption of the oxygen molecules on the metallic alloy substrate, their dissociative chemisorption, oxide nucleation and growth) into account. "Unit cells" of ⟨Al₂O₃⟩, ⟨MgO⟩ and ⟨MgAl₂O₄⟩ containing same molar quantities of oxygen and thus different molar quantities of oxide phases (due to their different metal-to-oxygen atomic ratios) are considered here. These corresponding oxidation reactions using per mole of O reactant are described as:

$$\frac{2}{3} \cdot Al(s) + \frac{1}{2} \cdot O_2(g) \rightarrow \frac{1}{3} \cdot \langle Al_2O_3 \rangle \tag{1}$$

$$Mg(s) + \frac{1}{2} \cdot O_2(g) \rightarrow \langle MgO \rangle \tag{2}$$

$$\frac{1}{4} \cdot Mg(s) + \frac{1}{2} \cdot Al(s) + \frac{1}{2} \cdot O_2(g) \rightarrow \frac{1}{4} \cdot \langle MgAl_2O_4 \rangle \tag{3}$$

Molar volumes per mole of O of these crystalline oxide overgrowths $\left(V_{(oxide)}\right)$ for 1-D oxide growth are given as:

$$V_{(oxide)} = h_{(oxide)} \times l_{(oxide)}^2 \tag{4}$$

where, $h_{(oxide)}$ and $l_{(oxide)}^2$ represent the oxide film thickness and its interface area, respectively (see Fig. 1), which leads to:

$$\frac{h_{(Al_2O_3)} \cdot l_{(Al_2O_3)}^2}{V_{(Al_2O_3)}} = \frac{h_{(MgO)} \cdot l_{(MgO)}^2}{V_{(MgO)}} = \frac{h_{(MgAl_2O_4)} \cdot l_{(MgAl_2O_4)}^2}{V_{(MgAl_2O_4)}} \tag{5}$$

The interface area of a "unit cell" is proportional to $V_{<oxide>}^{2/3}$. Thus, the interface area of ⟨Al₂O₃⟩ and ⟨MgAl₂O₄⟩ "unit cells" are related with respect to ⟨MgO⟩ "unit cell" as:

$$\frac{l_{(Al_2O_3)}^2}{l_{(MgO)}^2} = \frac{V_{(Al_2O_3)}^{2/3}}{V_{(MgO)}^{2/3}} \text{ and } \frac{l_{(MgAl_2O_4)}^2}{l_{(MgO)}^2} = \frac{V_{(MgAl_2O_4)}^{2/3}}{V_{(MgO)}^{2/3}} \tag{6}$$

Now to predict which of the crystalline oxide overgrowths is thermodynamically preferred, $G_{(oxide)}^{cell}$ of ⟨Al₂O₃⟩, ⟨MgO⟩ and ⟨MgAl₂O₄⟩ unit cells are compared per unit area of ⟨MgO⟩ unit cell (the ⟨MgO⟩ unit cell is arbitrarily chosen as the reference state). Expressions for $G_{(Al_2O_3)}^{cell}$, $G_{(MgO)}^{cell}$ and $G_{(MgAl_2O_4)}^{cell}$ become (see Eqs. (4)–(6)):

$$G_{(Al_2O_3)}^{cell} = \frac{l_{(Al_2O_3)}^2}{l_{(MgO)}^2} \cdot \left(h_{(Al_2O_3)} \cdot \frac{\Delta G_{(Al_2O_3)}^f}{V_{(Al_2O_3)}} + \gamma_{(AlMg)-(Al_2O_3)} + \gamma_{(Al_2O_3)-ambient} \right) \tag{7}$$

$$G_{(MgO)}^{cell} = h_{(MgO)} \cdot \frac{\Delta G_{(MgO)}^f}{V_{(MgO)}} + \gamma_{(AlMg)-(MgO)} + \gamma_{(MgO)-ambient} \tag{8}$$

$$G_{(MgAl_2O_4)}^{cell} = \frac{l_{(MgAl_2O_4)}^2}{l_{(MgO)}^2} \cdot \left(h_{(MgAl_2O_4)} \cdot \frac{\Delta G_{(MgAl_2O_4)}^f}{V_{(MgAl_2O_4)}} + \gamma_{(AlMg)-(MgAl_2O_4)} + \gamma_{(MgAl_2O_4)-ambient} \right) \tag{9}$$